Pressure-induced amorphization in crystalline silica: Soft phonon modes and shear instabilities in coesite

David W. Dean, Renata M. Wentzcovitch, N. Keskar, and James R. Chelikowsky
Department of Chemical Engineering and Materials Science, Minnesota Supercomputing Institute, University of Minnesota, Minneapolis, Minnesota 55455-0132

N. Binggeli
Institut de Physique Appliquée, Ecole Polytechnique Fédérale de Lausanne, 1015 Lausanne, Switzerland
(Received 1 March 1999; revised manuscript received 12 July 1999)

Quartz and closely related materials will transform under pressure from crystalline states to amorphous forms. Here we examine coesite, a high-pressure form of silica which also undergoes pressure induced amorphization. We find that coesite, like quartz, possesses a shear instability closely coupled to a zone-edge phonon softening at pressures comparable to the amorphization transformation. The commonality of these features strongly suggests that a coupling between a shear and a phonon soft mode plays an important role in pressure induced amorphization. This mechanism is similar to that observed in martensitic transformations. The densities for the phases produced at high pressures, as calculated from variable cell shape molecular dynamics, follow the experimental glassy region joining coesite to stishovite.

I. INTRODUCTION

Quartz and related materials such as berlinite ($AlPO_4$) will undergo a pressure-induced amorphization transformation at room temperature. The transformation can be sluggish and is not sharply defined.[1–4] Moreover, the driving mechanism for the transformation is not well understood. Suggested mechanisms for pressure induced amorphization in quartz have often focused on the existence of soft modes in the phonon spectrum coupled to a shear instability.[5,6] Calculations using pseudopotentials and interatomic potentials for quartz have resulted in the following scenario as a function of pressure. As the pressure increases, a softening of the lowest acoustic-phonon branch occurs. In particular, at modest pressures (~ 20 GPa) the entire acoustic branch exhibits a dispersion smaller than kT and the lowest mode at a zone edge becomes unstable. At this point, the acoustic branch is characterized by soft modes. The softening of this mode can be traced to an instability of the cation sites: the silicons can easily be displaced from tetrahedral sites to octahedral sites. This change in coordination is believed to occur via a rotation of the $Si(O_4)_{1/2}$ tetrahedral units in the pressure-induced amorphization transformation.[7] It is apparent that this mechanism will destabilize the quartz structure, but not necessarily indicate which structure quartz will assume.

There is both experimental and theoretical evidence for this picture. If a zone-edge softening occurs, one expects a possible pressure-induced crystal-to-crystal transformation will occur in quartz based on the soft mode at the zone edge.[7] This crystal-to-crystal transformation might precede the amorphization transformation as has been observed experimentally[2] and is consistent with the theoretical predictions.[7] Also, in an independent theoretical calculation,[8] it was noted that near the amorphization pressure a number of competing phases are possible. This finding is consistent with the existence of a soft phonon branch, i.e., it is possible for many modes to couple resulting in a large number of phases with similar energies. However, one can raise questions about the generality of this picture. For example, another crystalline phase of silica, coesite, also undergoes pressure-induced amorphization. One can ask whether the mechanism in quartz and coesite are similar. In particular, does coesite exhibit a zone-edge soft mode and an accompanying shear instability?

While quartz and coesite amorphize under pressure, the resulting disordered phase is not the lowest enthalpy form possible. A high-density form of silica, stishovite, is the thermodynamically stable phase above ~ 8 GPa. Stishovite is composed of edge sharing $Si(O_6)_{1/3}$ octahedra. This structure is one of the few naturally observed forms of silica that do not consist of a network of tetrahedra. The amorphous phases are of intermediate density and enthalpy between the low-density forms and stishovite. Direct transition to stishovite appears to be frustrated by a large free-energy barrier at low temperatures and high pressure. The glassy structures occur as kinetically accessible forms under these conditions.

II. STRUCTURE

Coesite is a high-pressure form of crystalline silica. Of the various silica polymorphs, coesite is the highest density tetrahedrally coordinated form. At ambient temperatures, coesite is more stable than quartz above 3.5 GPa. Also, coesite has a more complex crystal structure compared to quartz. It has a basis of 16 molecular units of SiO_2 in a monoclinic conventional unit cell that is nearly hexagonal.[9] It is possible, however, to chose a smaller unit cell. The lattice coordinates of one half of the atoms in the conventional cell can be generated from the other coordinates by a translation of $(\frac{1}{2},0,\frac{1}{2})$. Thus the conventional cell consists of two primitive cells. For efficiency, we use the primitive cell in our calculations. The primitive $(\mathbf{a}_{\mathbf{p}_i})$ and conventional $(\mathbf{a}_{\mathbf{c}_i})$ unit-cell vectors are

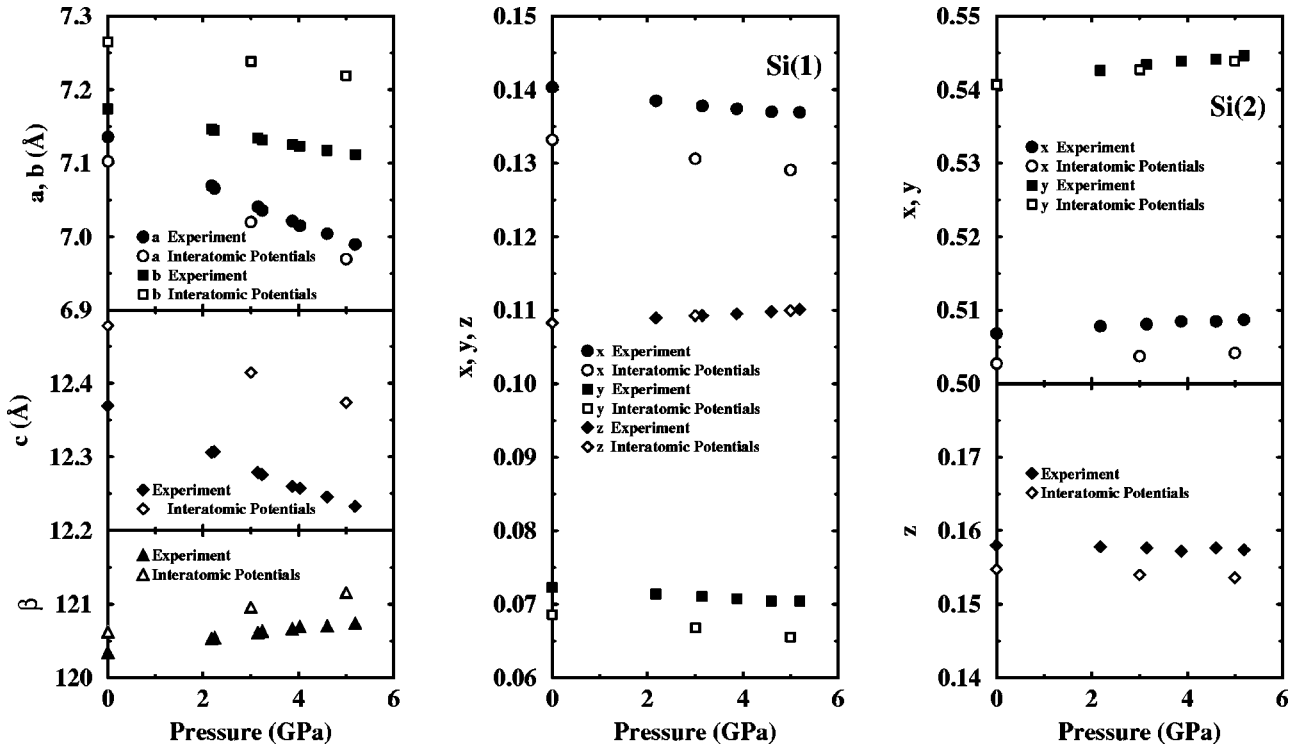

FIG. 1. Variation of conventional unit-cell parameters of coesite with pressure in GPa. Lattice vector lengths are in angstroms and angles in degrees. Open symbols are based on calculations with interatomic potentials. Measured data for coesite is indicated by filled symbols (Ref. 18).

$$\mathbf{a}_{\mathbf{p}_1}=\frac{1}{2}(\mathbf{a}_{\mathbf{c}_1}+\mathbf{a}_{\mathbf{c}_3})=\frac{1}{2}(a,-c,0), \tag{1}$$

$$\mathbf{a}_{\mathbf{p}_2}=\frac{1}{2}(\mathbf{a}_{\mathbf{c}_1}+\mathbf{a}_{\mathbf{c}_3})=\frac{1}{2}(a,c,0),$$

$$\mathbf{a}_{\mathbf{p}_3}=\mathbf{a}_{\mathbf{c}_2}=\mathbf{b}(\cos\gamma,\mathbf{0},\sin\gamma),$$

$$\mathbf{a}_{\mathbf{c}_1}=\mathbf{a}=\mathbf{a}_{\mathbf{p}_1}+\mathbf{a}_{\mathbf{p}_2}=\mathbf{a}(\mathbf{1},\mathbf{0},\mathbf{0}),$$

$$\mathbf{a}_{\mathbf{c}_2}=\mathbf{b}=\mathbf{a}_{\mathbf{p}_3}=\mathbf{b}(\cos\gamma,\mathbf{0},\sin\gamma),$$

$$\mathbf{a}_{\mathbf{c}_3}=\mathbf{c}=\mathbf{a}_{\mathbf{p}_1}-\mathbf{a}_{\mathbf{p}_2}=\mathbf{c}(\mathbf{0},-\mathbf{1},\mathbf{0}),$$

where γ is the angle between conventional unit-cell vectors **a** and **b**. In contrast, quartz has only three molecular units of SiO_2 within a hexagonal unit cell.

III. COMPUTATIONAL METHODS

Given the complexity of coesite, we have restricted our attention to a primitive cell and to interatomic pair potentials to characterize its structural and vibrational properties. We have chosen the following interatomic potentials after the work of van Beest and co-workers:[10,11]

$$u(r_{ij})=\frac{Z_iZ_je^2}{r_{ij}}+A_{ij}e^{-b_{ij}r_{ij}}-\frac{C_{ij}}{r_{ij}^6}, \tag{2}$$

where $u(r_{ij})$ is the interaction energy between atoms (i,j), r_{ij} is the interatomic separation, and $(Z_i,A_{ij},b_{ij},C_{ij})$ are parameters fit to Hartree-Fock calculations for the molecular fragments and experimental data for crystalline silica such as the elastic constants and structural data.

We will use these potentials to compute the phonon dispersion curves as a function of pressure in coesite and compare to quartz. The pressure evolution of the resulting phonon spectra describe the onset of structural instabilities. While we do not expect such pair potentials to reproduce the higher optical modes well, we expect that they will yield an accurate representation of the lowest phonon branches corresponding to structural instabilities. For example, in quartz we found that the group velocities calculated by interatomic potentials and quantum mechanically via pseudopotentials are essentially the same. Also, the interatomic potentials yield phonon frequencies for the lowest acoustic branches and elastic constants in good accord with experiment.[6,12]

The first step in this process is to equilibrate coesite to its ground-state structure as determined by the interatomic potentials. This has been done by choosing a series of pressures and relaxing the coesite structure for each one. This multivariable optimization process requires the minimization of a number of internal structural parameters along with the lattice constants.[13] The pressure can be determined by direct computation of the stresses from the interatomic potentials. Comparisons to measured lattice parameters are shown in Fig. 1. These potentials yield reasonable agreement for the measured lattice constants, e.g., the lattice parameters agree to within 2–3%. The *x*, *y*, and *z* coordinates of Si reflect the arrangement of the $Si(O_4)_{1/2}$ tetrahedra.

For each pressure configuration, we may obtain the phonon spectra from the eigenvalues of the dynamical matrix **D**:

$$\mathbf{D}(\mathbf{k})\mathbf{w}=-\omega^2(\mathbf{k})\mathbf{w}, \tag{3}$$

where the reduced displacement of atom m along direction i is given by $w_{mi}=M_m^{1/2}(r_{mi}-r_{mi}^0)$. The atomic equilibrium positions are $\mathbf{r_m^0}$ and the mass of the mth atom is M_m. The elements of $\mathbf{D}$ are given by

$$D_{mnij}(\mathbf{k})=\frac{1}{\sqrt{M_m M_n}}\sum_l \frac{\partial F_{mi}}{\partial r_{nlj}} e^{-i2\pi\mathbf{k}\cdot(\mathbf{R_l}+\mathbf{r_n}-\mathbf{r_m})}, \quad (4)$$

where F_{mi} is the force on atom m along direction i, $\mathbf{k}$ is the phonon wave vector, the subscript l refers to lattice vector $\mathbf{R_l}$, and r_{nlj} is the component of $\mathbf{r}$ along the $\mathbf{j}$ direction for the nth atom in the lth unit cell. The partial derivative of the force is evaluated at the equilibrium positions. The forces on each atom can easily be computed from the interatomic potentials. The summation in Eq. (4) is carried out to a radius of approximately 40 Å. Imaginary frequencies in the resulting phonon spectra indicate structural instabilities and are associated with spontaneous structural transitions.

Once a system crosses into a pressure regime that produces structural instability, it will follow a trajectory in configuration space that will eventually violate the harmonic approximation inherent in the phonon calculation. To predict such trajectories requires a molecular-dynamics method that can account for variations of the unit-cell shape as well as the motions of the constituent atoms. Our combined atom and cell dynamics are based on an approach developed by Wentzcovitch.[13]

Finite temperature, zero-point motion, and tunneling can add random motions to the system trajectory and allow the system to escape from local energy minima in configuration space. To account for such effects, we use molecular dynamics to perform simulate annealing. The equations of motion governing the motion of the atoms and variations in unit-cell shape must be combined with some means of controlling the temperature of the system. Rather than add random forces to impose thermal equilibrium with a reservoir, we periodically rescale the velocities in order to reset the total kinetic energy to $(3N-3)k_BT/2$.

IV. PHONON SPECTRA

Prior to examining coesite, we had already investigated the phonon spectra of quartz and its evolution with pressure.[6] In Fig. 2 we illustrate the lowest acoustic branches in α quartz at a pressure of 22 GPa. The dispersion shown is along the Γ to K direction in the quartz Brillouin zone where the instability occurs.[5,6] The width of the lowest branch is only about 1 THz. We believe this soft mode is triggering a sequence of transformations leading to the amorphization. In most open forms of silica, including quartz and coesite, the cations reside in tetrahedral sites, but in more dense forms such as stishovite, the cations reside in octahedral sites. Under pressure, the fourfold sites become destabilized versus the sixfold sites.

Here we perform similar calculations for coesite. On the left-hand side of Fig. 3, we illustrate phonon modes for coesite along several high symmetry directions as a function of pressure. We find that as the pressure is increased an instability arises at the zone center. In particular, at the zone center, the lowest branch becomes imaginary near 8 GPa. At this point, the coesite structure will spontaneously distort.

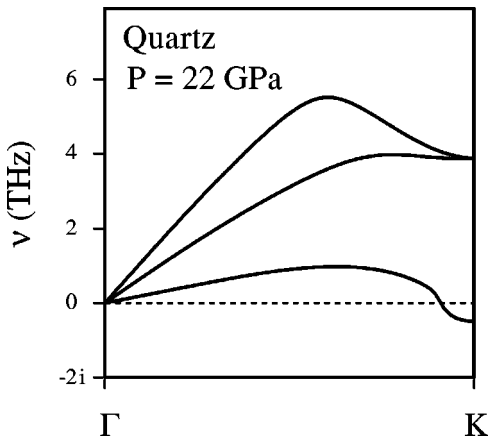

FIG. 2. Lowest phonon branches in quartz at a pressure of 22 GPa. The lowest acoustic branch becomes imaginary near the zone edge.

However, if the calculations are continued at higher pressure ($\sim$20 GPa), with the fixed coesite symmetry, the group velocity corresponding to the slope of the lowest acoustic branch at the zone center becomes strongly imaginary. This trend would appear to be at variance with the instability observed in quartz. In quartz, the zone-edge phonon softens in concert with the zone-center instability. In coesite, the zone center becomes unstable at much lower pressures ($\sim$10 GPa in coesite versus $\sim$25 GPa in quartz) and there appears to be no zone-edge softening.

It should be noted, however, that in the case of zone-center softening, the structural changes one expects do not correspond to a new crystal phase *per se*, but rather a distortion of the unit-cell shape. To stabilize the structure at higher pressures, we allowed the coesite unit cell to distort by minimizing enthalpy with respect to changes in the lattice parameters and atom coordinates. At 20 GPa, we found relatively small changes of less than a few percent in the lattice parameters.[14] The density change from the ideal to the distorted coesite structure was less than 1.3%. In the ''distorted coesite'' structure, the zone-center instability is removed.

Using the optimized lattice parameters and internal coordinates of the distorted coesite structure, we calculated the phonon dispersion curves from 10 to 24 GPa. The calculated phonon spectra for this distorted structure are shown on the right-hand side of Fig. 3. Strictly speaking, the distorted structure is triclinic. For comparison purposes, we calculated the phonon spectra along the same directions in reciprocal-lattice coordinates as used for the coesite structure. The small distortion of the coesite structure splits the degeneracy of the lowest branch along the A to H direction. The lower of the two branches softens with pressure and at about 24 GPa vanishes at the zone boundary. The width of this branch is $\sim$1 THz which is similar to that of the corresponding soft branch in quartz (Fig. 2). The existence of soft phonon mode at $\sim$24 GPa is consistent with the pressure observed for the onset of the amorphization transformation of coesite. However, the softening of the zone center mode is weaker than in quartz.

The existence of a zone-edge soft mode suggests that coesite may also have a crystal$\rightarrow$crystal transformation which accompanies or precedes the amorphization transformation.

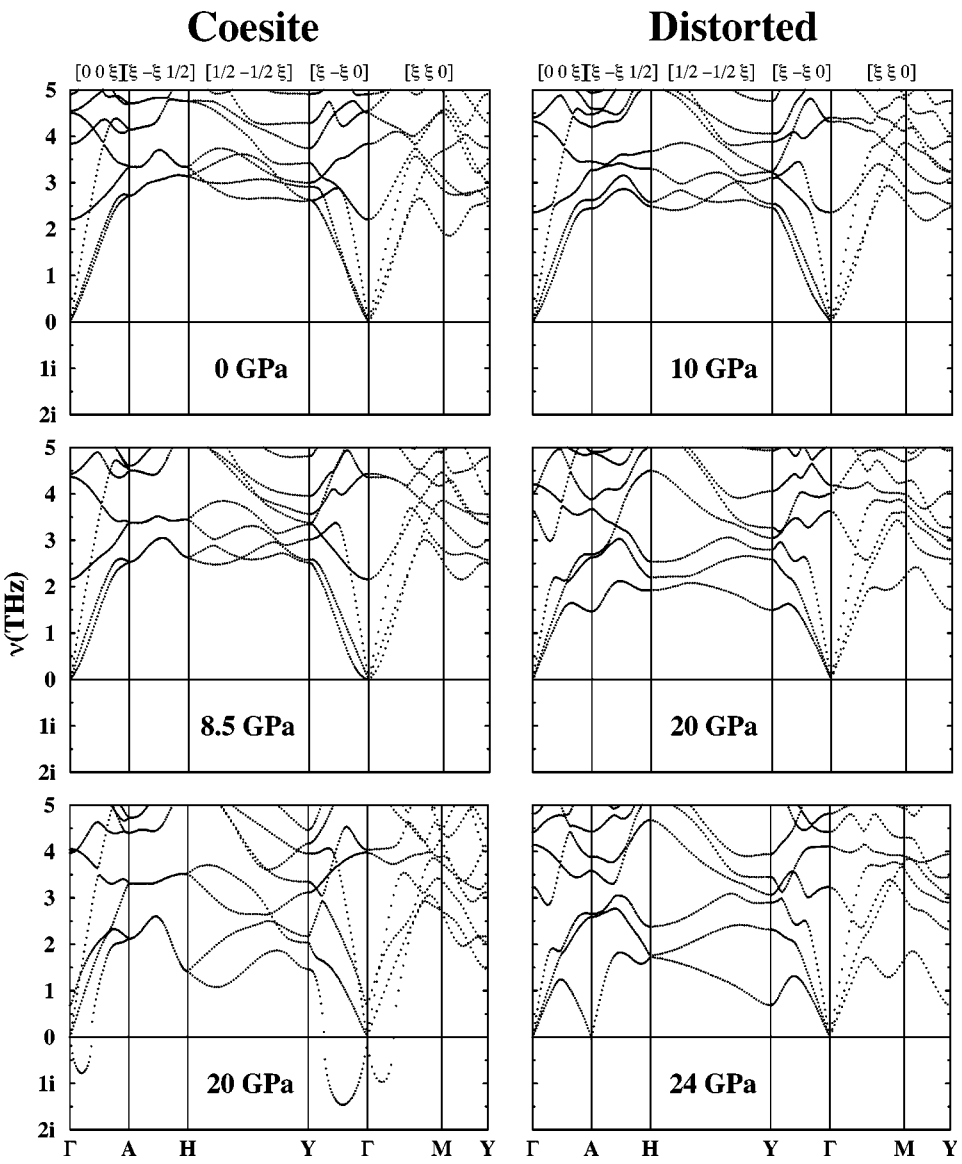

FIG. 3. Phonon branches for coesite and the ''distorted'' coesite structure (see text). Several pressure regimes are illustrated. The symmetry of coesite is preserved for the spectra shown on the left, and the structure relaxed from coesite for the spectra on the right.

There is some evidence for this in recent work.[15] We also note the similarity of such shear and zone-edge soft modes in quartz and coesite to our earlier work on $AlPO_4$ (berlinite).[16] Berlinite is isostructural with quartz. Its phonon spectrum under pressure is quite similar; it also undergoes a pressure-induced amorphization.[4]

While soft shear and phonon modes are present in all these materials, the pressure at which the phonon instabilities occur are not entirely consistent with experiment. For example, in berlinite the instability does not occur until almost 35–40 GPa or about 20 GPa above the observed transformation pressure.[16] Anharmonic effects, including phonon shear and phonon-phonon couplings have not been included in our analysis. These higher-order corrections could further destabilize the coesite structure and decrease the transition pressure. In general, however, such couplings decrease the transitions pressure by no more than a few GPa.[17] Also, the shear and zone-edge instabilities are separated by about 15–20 GPa in berlinite and coesite in contrast to quartz where the two pressures differ by ~5 GPa. We do not attach any particular weight to these differences as we do not expect such ''details'' to be accurately described by simple pair potentials.

V. MOLECULAR-DYNAMICS SIMULATIONS

The existence of a lower enthalpy configuration is a necessary, but not sufficient, condition for a phase transition at constant pressure. A kinetically accessible path in phase space must be available for the transition to proceed. Total-energy calculations are required to predict the relative enthalpies of possible structures. Stability criteria based on the phonon spectra can only indicate the initial trajectory associated with the phase transition. The equations of motion of the nuclei must be integrated, i.e., molecular dynamics (MD), to follow the trajectory to a final stable structure. Local enthalpy minima can be overcome by adding kinetic energy to the system to simulate finite temperature.

In principle, at pressures where imaginary phonon modes with finite wavelengths exist, a sufficiently large simulation cell should spontaneously undergo a structural transformation. We examined this behavior for this zone-edge instability above 24 GPa. The wave vector associated with the zone edge at A corresponds to two primitive unit cells repeated along the lattice vector a_{p_3}. A supercell consisting of two such primitive unit cells spans exactly one full wavelength of this phonon. This MD simulation cell should exhibit struc-

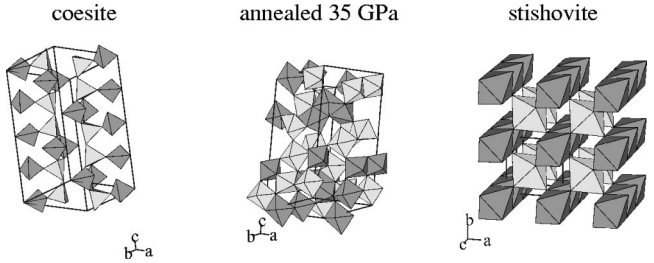

FIG. 4. Coesite supercell consisting of $1\times1\times2$ conventional unit cells (left), annealed structure at 35 GPa (center), and $2\times2\times2$ unit cells of stishovite (right). The polyhedra correspond to $Si(O_4)_{1/2}$ and $Si(O_6)_{1/3}$ units.

tural instability at this pressure and can be used to explore possible new structures.

Starting with a supercell composed of $1\times1\times2$ primitive unit cells, we perturbed the system from the coesite structure with displacements corresponding to the A phonon eigenmode. We then relaxed at 0 K to minimize enthalpy. In order to overcome the local energy barriers and facilitate transition to a lower enthalpy structure, we followed the relaxations with a simulated annealing. Starting with the relaxed structure, we allowed the system to equilibrate at 1200 K (well below the melting temperature of $\sim$3000 K) for 1050 time steps of 2.9 fs each. The temperature was then lowered by 200 K increments and held for 1000 time steps at each temperature. The temperature was maintained by rescaling the total kinetic energy every 50 time steps. At 0 K, the cell parameters and atomic coordinates were relaxed to minimize enthalpy for the final structure. We also performed similar simulations at 10 and 20 GPa, i.e., below the pressure of the zone-edge instability, using a supercell which can accommodate the soft shear and a phonon modulation with a wave vector halfway along $\Gamma-Y$.

It is interesting to note that coesite becomes metastable with respect to stishovite for pressures near 8 GPa at ambient temperatures. This pressure at which the zone center instability in coesite appears is consistent with the coesite-stishovite phase boundary observed experimentally.[3] However, given the uncertainties in the interatomic potentials, and the fact that the coesite phase can persist well above the phase boundary pressure, this may be a coincidence. The simulated anneal at 10 GPa produced a final structure that remained a minor distortion of the coesite structure, as obtained from the simple relaxation calculations. At higher pressures a dramatic collapse of the structure occurred. An example of the final structure at 35 GPa is shown in Fig. 4 along with the coesite and stishovite structures. The density and enthalpies are brought closer to stishovite as indicated in Table I. Even though the potential energy of the system is above that of coesite, this increase is more than compensated by the density increase and associated pV work term.

In Fig. 5 we display the radial and angular distribution functions of the final structures at 20, 25, and 35 GPa, and compare them to those of coesite and stishovite. These distribution functions clearly illustrate the intermediate nature of the annealed structures. Under compression, the tetrahedra rotate about the oxygen vertices, as seen in the more acute Si-O-Si angles obtained for the high-pressure structures. These rotations bring non-nearest-neighbor oxygens closer to the silicons, as reflected in the Si-O radial distribution function. The lower tail of the distribution above 4 a.u. (1 a.u. $=0.529$ Å) in Fig. 5 extends to the nearest-neighbor region and increases the average coordination. The distortion of the silicon-centered polyhedra in these intermediate structures can be seen in the O-Si-O angular distribution functions. The O-Si-O angles in coesite are tightly clustered around the ideal 109° for perfect tetrahedra. Stishovite has Si-O-Si angles near 90° and 180° associated with a perfect octahedron. The annealed structures appear to break up the coesite distribution toward these two groups near 90° and 180°. The annealed structures in Fig. 4 clearly evolve towards the stishovitelike octahedral arrangement of the O atoms about the Si atoms. However, the structures lack the ordered arrangement of these octahedra as is present in stishovite. These structures produce distributions that are sequentially intermediate between coesite and stishovite.

TABLE I. Predicted energy, work, enthalpy, and density relative to stishovite.

	Energy	pV (kJ/mole)	Enthalpy	Density (g/cm^3)
20 GPa				
Coesite	22.7	102.6	125.2	3.28
Relaxed and annealed	50.4	56.9	107.3	3.75
Stishovite	0.0	0.0	0.0	4.56
25 GPa				
Coesite	29.8	120.2	150.0	3.37
Relaxed and annealed	71.0	32.9	103.9	4.18
Stishovite	0.0	0.0	0.0	4.61
30 GPa				
Coesite	37.5	135.8	173.4	3.44
Relaxed and annealed	80.6	37.6	118.2	4.24
Stishovite	0.0	0.0	0.0	4.65
35 GPa				
Relaxed and annealed	92.4	15.5	108.0	4.53
Stishovite	0.0	0.0	0.0	4.69

The equations of state for coesite, stishovite, and amorphous phases are illustrated in Fig. 6, and compared to available experimental data. The two sets of experimental data for coesite[1,18] have been fit to a third-order Birch-Murnaghan equation. The molar volumes for coesite based on interatomic potentials falls slightly above this equation. Those molar volumes calculated for stishovite fall on the extrapolated equation of state for stishovite.[19] The possible range of volumes for glassy silica as fit by Hemley[1] is shown in gray. The densities of our annealed structures above 10 GPa are in striking agreement with the corresponding region of amorphous phases joining coesite and stishovite in the pressure-volume diagram. This result indicates that, in spite of their simplicity, the interatomic potentials capture the main features of the coesite phase transformations under pressure.

VI. CONCLUSIONS

With respect to the driving mechanisms of the high-pressure amorphization transformations, the commonality of

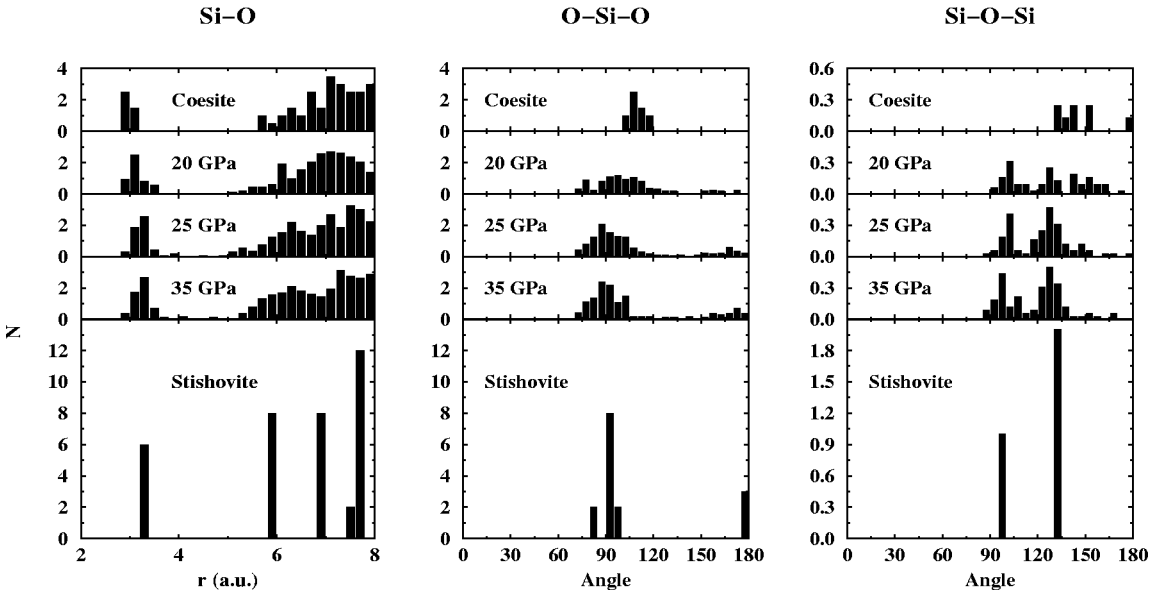

FIG. 5. Radial and angular distribution functions of coesite, annealed structures, and stishovite. The histograms represent the average number of oxygen atoms per silicon within 0.2 a.u. (1 a.u.$=0.529$Å) or 5° intervals for the radial and angular distributions, respectively.

the soft shear and zone-edge instability found here in coesite and previously in berlinite and quartz suggests that a coupling between a shear and a zone-edge phonon mode may play an important role in these transformations. Such a mechanism is quite similar to the apparent driving mechanism of martensitic transformations in metallic alloys, where a shear mode couples to a soft phonon mode.[20] In metallic shape-memory alloys, such a coupling gives rise to microstructures with different crystallographic orientations corresponding to equivalent shear planes. These martensitic microstructures are responsible for the shape-memory effect as they all revert to the same, singly oriented, parent phase when the temperature is increased.[21] Here the systems are quite different, but a similar mechanism appears to play an important role. In particular, experiments suggest that berlinite is a memory glass: it amorphizes under pressure, but when the pressure is released it returns to a crystalline state with same orientation as before pressure was applied.[4] In the case of quartz, the recovered material appears amorphous under x-ray measurements, but displays anisotropic elastic properties indicating that some memory of the initial crystal orientation has been retained.[22] Such similarities in the driving forces and observed behavior suggest that martensitic microstructures, accompanying or preceding the amorphization transformation, may also be largely responsible for the memory effects reported in quartz and related materials.

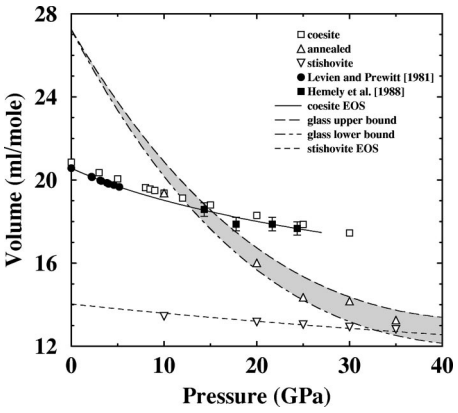

FIG. 6. Molar volume (ml/mole) dependence on pressure (GPa) for coesite, stishovite, and intermediate phases of silica. The open squares, diamonds, triangle (pointed up), and inverted triangles are based on calculations with interatomic potentials for coesite, annealed structures, and stishovite, respectively. Measured data for coesite are indicated by filled circles (Ref.18) and squares (Ref. 1). The equation of state (EOS) for coesite is fit from both sets of data (Ref. 1). The upper (long dash line) and lower (dashed and dotted line) bounds for glass were taken from polynomial fits of Hemley *et al.* (Ref. 1). The equation of state for stishovite (short dash line) is extrapolated from Bass *et al.* (Ref. 19).

The compressed structures based on molecular-dynamics simulations exhibit features intermediate to coesite and stishovite. The radial distribution functions of O atoms about Si atoms show the coordination increasing with pressure from the value of 4 for coesite to nearly 6 associated with stishovite. The bond angle distribution functions reflect the rotation of the network tetrahedra to form the stishovitelike octahedra.

The ability of interatomic potentials to reproduce the structures of the crystalline silica polymorphs has long been established. Our results show that the disordered phases produced by high pressure and the processes leading to them, are also well characterized by the same interatomic potentials. The variation of density of amorphous silica at high pressure is accurately reproduced by our calculations.

ACKNOWLEDGMENTS

We would like to acknowledge support for the work from the Minnesota Supercomputing Institute. Two of us (D.W.D. and J.R.C.) would like to acknowledge support from the U.S. Department of Energy (Grant No. DE-FG02-89ER45391). R.M.W. acknowledges support from the National Science Foundation (Grant No. EAR-9628042). J.R.C. also acknowledges support from the Miller Institute.

[1] R.J. Hemley, A.P. Jephcoat, H.K. Mao, I.C. Ming, and M.H. Manghnani, Nature (London) **334**, 52 (1988).
[2] K.J. Kingma, R.J. Hemley, H.K. Mao, and D.R. Veblen, Phys. Rev. Lett. **21**, 3927 (1993).
[3] R.J. Hemley, C.T. Prewitt, and K.J. Kingma, in *Silica: Physical Behavior, Geochemistry and Materials Applications*, edited by P.J. Heaney, C.T. Prewitt, and G.V. Gibbs, Reviews in Mineralogy Vol. 29 (Mineralogical Society of America, Washington, DC, 1994), p. 41.
[4] M.B. Kruger and R. Jeanloz, Science **249**, 648 (1990).
[5] S.L. Chaplot and S.K. Sikka, Phys. Rev. B **47**, 5710 (1993).
[6] N. Binggeli and J.R. Chelikowsky, Phys. Rev. Lett. **71**, 2674 (1993); **69**, 2220 (1992).
[7] R.M. Wentzcovitch, C. da Silva, J.R. Chelikowsky, and N. Binggeli, Phys. Rev. Lett. **80**, 2149 (1998).
[8] D.M. Teter, R.J. Hemley, G. Kresse, and J. Hafner, Phys. Rev. Lett. **80**, 2145 (1998).
[9] L. Levien, C.T. Prewitt, and D.J. Weidner, Am. Mineral. **65**, 920 (1980).
[10] B.W.H. van Beest, G.J. Kramer, and R.A. van Santen, Phys. Rev. Lett. **64**, 1955 (1990).
[11] G.J. Kramer, N.P. Farragher, B.W.H. van Beest, and R.A. van Santen, Phys. Rev. B **43**, 5068 (1991).
[12] N. Binggeli, J.R. Chelikowsky, and R.M. Wentzcovitch, Phys. Rev. B **49**, 9336 (1994).
[13] R.M. Wentzcovitch, Phys. Rev. B **44**, 2358 (1991).
[14] The lattice parameter c increased by less than 0.3%, b decreased by $\sim 2\%$, and a remained unchanged. The angles (α,β) changed from 105° to 107° and 103°, respectively. The γ angle remained unchanged at 122°. See Ref. 9 for structural details of coesite.
[15] R.J. Hemley, *High-Pressure Research in Mineral Physics*, edited by M.H. Manghnani and Y. Syono (Terra Scientific, Tokyo, Am. Geophys. Union, Washington, DC, 1987), p. 347.
[16] N.R. Keskar, J.R. Chelikowsky, and R.M. Wentzcovitch, Phys. Rev. B **50**, 9072 (1994); Also see, J.S. Tse and D.D. Klug, Science **255**, 1559 (1991).
[17] M.B. Nardelli, S. Baroni, and P. Giannozzi, Phys. Rev. Lett. **69**, 1069 (1992).
[18] L. Levien and C.T. Prewitt, Am. Mineral. **66**, 324 (1981).
[19] J.D. Bass, R.C. Liebermann, D.J. Weidner, and S.J. Finch, J. Phys. Earth **25**, 140 (1981).
[20] Y.Y. Ye, C.T. Chan, K.M. Ho, and B.N. Harmon, Int. J. Supercomput. Appl. **4**, 111 (1990); Y.Y. Ye, C.T. Chan, and K.M. Ho, Phys. Rev. Lett. **66**, 2018 (1991).
[21] See articles, in *Shape Memory Materials*, edited by K. Otsuka and C. M. Wayman (Cambridge University Press, Cambridge, 1998).
[22] L.E. McNeil and M. Grimsditch, Phys. Rev. Lett. **68**, 83 (1992); **72**, 1301 (1994); K.J. Kingma, R.J. Hemley, H.K. Mao, and D.R. Veblen, *ibid.* **72**, 1302 (1994).